Structural Characterization of Lignin Isolated from Wheat-Straw during the Alkali Cooking Process

Xiaojun Tian,[a,#] Bing Wang,[b,#] Bin Wang,[a,*] Jinpeng Li,[a] and Kefu Chen [a]

To investigate the behavior of lignin during the alkali cooking process with different alkali doses, this work demonstrated the structural characteristics illustrated by spectroscopic analyses. Gel permutation chromatography (GPC) and nuclear magnetic resonance (NMR) indicated that the lignin was composed of typical structures for a grass, generally with S and G units and small amounts of H units. The main substructures present were β-*O*-4 aryl ether linkages, and there were lower amounts of β-β and β-5 linkages. Alkali treatment conditions had evident effects on the chemical structures and properties of lignin. Moreover, NMR indicated that alkali cooking caused lignin to depolymerize more easily with increasing severity and to condense.

Keywords: Alkali cooking; Lignin; Structural characterization; Wheat-straw

Contact information: a: Plant Micro/Nano Fiber Research Center, State Key Laboratory of Pulp and Paper Engineering, School of Light Industry and Engineering, South China University of Technology, Guangzhou 516640, China; and b: Beijing Key Laboratory of Lignocellulosic Chemistry, Beijing Forestry University, Beijing, 100083, China;
** Corresponding author: febwang@scut.edu.cn; # Contributed equally to this work*

INTRODUCTION

With the inevitable depletion of fossil fuels and increasing environmental concerns, lignocelluloses, such as agricultural and forest residues, are viewed as sustainable alterative resources for producing liquid fuels and chemicals because of their abundance and sustainability (Balat and Balat 2009; Lu and Ralph 2011). The main components of lignocellulosic biomass are cellulose, hemicelluloses, and lignin, and these biopolymers can be converted to biofuels (bioethanol) and bio-based chemicals by employing either a thermo-chemical or biological approach (Boateng *et al.* 2008).

Traditionally, cellulose fibers are used to produce pulp, paper, and bioethanol. Cellulose fibers are chemically or mechanically separated from lignocelluloses such as wheat straw. It is considered as a suitable raw material for pulp and biofuels production, owing to its characteristics, such as annual, abundance, renewability, and high-sugar content (Saini *et al.* 2015). Meanwhile, plentiful amounts of lignin are generated as a by-product with modified and degradative structures in the pulping technology, for example: alkali cooking, which is one important process (Stark 2011). As the second most abundant natural polymer, lignin accounts for 25% to 30% of biomass. It is the only renewable source of aromatic compounds for the chemical industry, and it presents both a significant opportunity and many challenges for enhancing the operation of a lignocellulosic biorefinery (Tuck *et al.* 2012; Upton and Kasko 2015). Its potential, however, is currently underutilized. Approximately 2% of the lignin extracted from pulping processes is used for high-value products, while the rest is burned as a low-value fuel (Stewart 2008; Liu *et al.* 2012; Kumar and Murthy 2013).

Structural information of lignin is particularly important for evaluating its utilization. Understanding of lignin structural features will facilitate lignin recovery and enable catalytic modifications to obtain desired chemicals and physical properties (Duval and Lawoko 2014). Lignin is a structurally complex polyphenolic biomacromolecule consisting primarily of three basic structural phenylpropane units: syringyl (S), guaiacyl (G), and *p*-hydroxyphenyl (H). Lignin is composed of different substructures, including the ether (β-*O*-4, α-*O*-4, and 4-*O*-5) and C-C linkages (β-β, β-5, β-1, and 5-5), and the proportion of *β-O*-4 linkages of the lignin obviously affects the distribution of degraded products and yield of depolymerized monomeric products (Bouxin *et al.* 2015). Each of these substructures varies according to the biological species and the chemical method used for its extraction (Zhang *et al.* 2016).

Lignin plays an important role in defense and water transport in vascular terrestrial plants (Zeng *et al.* 2013). Agricultural residues, such as cereal straws, are potential materials for the pulp and paper industry because their major constituents are comparable to wood species. In particular, wheat straw is used extensively as a raw material for pulp and paper. Generally, a large amount of lignin is generated during the pulping process, and both the structure and the chemical properties are modified. Therefore, it is essential to analyze the structure of lignin that is extracted from the pulp residues of wheat straw.

Several methods have been developed to separate lignin from lignocellulosic biomass, including chemical (dilute acid or alkali, organosolv, and ionic liquid), physical (mechanical extrusion), physico-chemical (steam explosion), and biological (white and soft rot fungi) (Kapoor *et al.* 2015). Alkaline treatment is the most widespread and cost-effective method for isolating lignin (mainly alkali lignin). Generally, alkali pretreatment involves the use of bases, such as sodium, potassium, calcium, and ammonium hydroxide, leading to lignin extraction by breaking hydrogen and other covalent bonds. Mild alkaline treatment, such as aqueous NaOH, causes the slight destruction of lignin structures that have relatively small molecular weight and still contain appreciable amounts of phenolic hydroxyl groups. Although the lignins in wood and non-wood plants share the basic chemical structure, the structural properties of gramineae lignin differ from those of softwood or hardwood lignins. For instance, the lignins isolated from graminaceous plants contain hydroxycinnamic acids, such as *p*-coumaric and ferulic acids (Sun *et al.* 2000b; Sun and Tomkinson 2002).

In most of the current pulping technologies, delignification consists of degradation and dissolution, which cleaves the native lignin into soluble fragments to separate it from the fibers (Gandini 2008). The important reactions during the alkaline pulping include the cleavage of phenolic α-*O*-4 linkages and non-phenolic β-*O*-4 linkages, and the removal of residual lignin fractions by cleavage of carbon-carbon linkages or by carbohydrate degradation, releasing lignin-carbohydrate fractions (Sun *et al.* 2000a). Though lignin has a negative impact on paper manufacturing, it has shown potential in other areas, such as a constituent of polymeric materials and in chemicals (Wang *et al.* 2016).

This study investigated the detailed chemical changes taking place in wheat straw lignin when wheat straw was cooked with varying concentrations of sodium hydroxide and sodium sulfide. The effect of temperature on the structural features of lignin was also analyzed. The structural information of the lignin fractions obtained was investigated by gel permeation chromatography (GPC), quantitative ^{13}C, two-dimensional heteronuclear single-quantum coherence (2D-HSQC), and ^{31}P nuclear magnetic resonance (NMR) spectroscopy.

EXPERIMENTAL

Materials

Wheat straw was provided by Shandong Tranlin Group Co., Ltd. (Shandong, China). The material was cut into pieces (approximately 20 mm long) and washed with tap water to remove soil particles. The washed wheat straw was air-dried and stored in a self-sealing plastic bag. Solid alkalis of sodium hydroxide and sodium sulphide powder with a purity of over 96.0% were purchased from Tianjin Kermel Reagent Co. Ltd., Tianjin, China. Deuterated dimethyl sulfoxide (DMSO- d_6) with a purity of over 99.9% was obtained from Sigma-Aldrich (Shanghai, China).

Water (18.2 MΩ) was purified with a Millipore Milli-Q system (Millipore Direct-Q5, Billerica, MA, USA). All other analytical reagent grade chemicals were obtained from Sinopharm Chemical Reagent Co. (Shanghai, China) and used without further purification.

Alkali Cooking Process

Twenty-five g dried wheat straw were loaded into a horizontal rotary digester (KRK 2611, Kyoraku Co. Ltd., Osaka, Japan) with a liquid/solid ratio of 10:1 (w/w). The added proportion of sodium hydroxide and sodium sulphide (based on oven-dried (od) raw material) was according to the cooking conditions as listed in Table 1.

The cooker was sealed, heated to 155 °C with a heating rate of 1 °C/min, and held at the target temperature (Table 1) for 30 min. When the cooking process completed, the black liquor was collected by filtration with an 80-mesh screen.

Table 1. Parameters of Alkali Cooking

Group	Sodium Hydroxide Dosage (%)	Sulfidity (%)	Heating Time (min)
L_1	6	14	120
L_2	8	14	120
L_3	10	14	120
L_4	12	14	120
L_5	14	14	120
L_6	10	6	120
L_7	10	10	120
L_8	10	14	120
L_9	10	16	120
L_{10}	10	18	120
L_{11}	10	14	60
L_{12}	10	14	80
L_{13}	10	14	100
L_{14}	10	14	120
L_{15}	10	14	140

Precipitation of Lignin

The black liquor was concentrated to approximately 30 mL using rotary evaporation, and 90 mL ethanol was added into the concentrated black liquor to ensure the ethanol concentration up to 70%. The sediment was removed by a G2 glass sand funnel filter, and the filtrate was concentrated to 10 mL. To completely precipitate the lignin, the solution was adjusted to pH 2 by slowly adding hydrochloric acid (1 mol/L). The

precipitate was washed with deionized water to a neutral pH and collected by centrifugation at 10000 rpm for 10 min. After separation and purification, the resultant lignin was dried into powder at 40 °C for 24 h.

Analysis Procedures

The associated polysaccharides in lignin were determined using high performance anion exchange chromatography (HPAEC) as reported previously (Sun *et al.* 2014). The weight-average (M_w) and number-average (M_n) molecular weights of the lignin fractions were determined by GPC, which were based on the procedures described in a previous literature (Sun *et al.* 2014). A PL-gel 10 mm mixed-B 7.5 mm i.d. column (Polymer Laboratories, Amherst, MA, USA) was calibrated with PL polystyrene standards. The lignin samples (2 mg) without acetylation were dissolved in 4 mL of tetrahydrofuran (THF), and 20 μL lignin solutions were injected. The solution-state NMR spectra of the lignin samples were acquired on a 400 MHz NMR spectrometer (AVIII 400, Bruker, Karlsruhe, Germany) at 25 °C using 140 mg of lignin in 0.5 mL of DMSO-d_6 for ^{13}C NMR spectra and 40 mg of lignin in 0.5 mL of DMSO-d_6 for HSQC NMR spectra (Holtman *et al.* 2006; Rencoret *et al.* 2008). ^{31}P-NMR spectra were used to detect the functional groups (aliphatic hydroxyl, phenolic hydroxyl, and carboxyl groups) of the lignin as previously described (Granata and Argyropoulos 1995).

RESULTS AND DISCUSSION

Associated Polysaccharides of the Lignin Fractions

To verify the purity of the lignin extracted from the wheat straw, the associated polysaccharides of the lignin samples were determined by HPAEC (Table 2). The five lignin samples contained a low amount of associated polysaccharides, ranging from 0.47% to 1.22%, implying that the lignin had a higher purity. Glucose (0.26% to 0.65%) and xylose (0.15% to 0.65%) were the major sugar constituents of the five lignin fractions. Arabinose was identified as a minor sugar constituent, and galactose was only detected in L_3. In addition, glucuronic and galacturonic acids were not detected in any lignin fractions. The glucose content decreased with increasing temperature. In contrast, xylose content increased with elevating temperature. Furthermore, the amount of total sugars decreased as the alkali concentration and temperature increased, suggesting that the ether and ester linkages between lignin and hemicelluloses in the cell walls of wheat straw were cleaved under the conditions given.

Table 2. Contents of Associated Polysaccharides of the Lignin Fractions Obtained from Wheat Straw

Lignin	Arabinose	Galactose	Glucose	Xylose	Total sugars[a]
L_1	0.20	ND[b]	0.65	0.37	1.22
L_3	0.27	0.13	0.35	0.45	1.20
L_5	0.33	ND	0.26	0.82	1.41
L_{11}	0.12	ND	0.32	0.21	0.65
L_{13}	ND	ND	0.28	0.19	0.47

[a] Represents the total associated carbohydrates in the lignin fractions (% dried lignin)
[b] ND, not detected

Molecular Weight Analysis of the Lignin Fractions

The weight-average (M_w), number-average (M_n) molecular weights, and polydispersity (M_w/M_n) of the lignin fractions were obtained by GPC (Table 3). The increase of alkaline concentration from 6 to 10% led to the increase of M_w from 2140 to 2510 g/mol. The reason for this increase may be that higher content of S-type lignin fractions were extracted, as evidenced by the 2D-HSQC NMR spectra. However, as the alkaline concentration further increased to 14%, the M_w of lignin (L_5) then decreased to 1740 g/mol, suggesting that the depolymerization possibly occurred at a relatively high alkaline concentration. With the extension of time from 60 to 100 min, the M_w of the lignin increased from 2150 to 3080 g/mol. However, the M_w of lignin (L_3) then decreased to 2510 g/mol as the time extended to 120 min. The diversified reason was possibly that the depolymerization and repolymerisation occurred under the special conditions. In other words, depolymerization and repolymerisation of lignin were competitive reactions. The depolymerization was the dominant reaction at relatively mild conditions. In contrast, the critical role of the repolymerization on the extraction of lignin occurred at severe conditions (high temperature and high alkali concentration).

Table 3. Weight-Average Molecular Weight (M_w), Number-Average (M_n) Molecular Weight, and Polydispersity (M_w/M_n) of Lignin Fractions

Sample	L_1	L_3	L_5	L_{11}	L_{13}
M_w	2140	2510	1740	2150	3080
M_n	1330	1320	840	1230	1660
M_w/M_n	1.60	1.90	2.07	1.76	1.86

Quantitative ^{13}C-NMR Analysis

To understand the structural transformation of the lignin fractions during the pretreatment process, quantitative ^{13}C-NMR spectra of L_1, L_3, and L_9 were recorded (Fig. 1), and the detail assignments were conducted according to previous publications about the NMR characterization of lignin (Martínez *et al.* 2008; del Río *et al.* 2009). The region between 104.4 and 168.2 ppm represents the aromatic group of the lignin, displaying the basic lignin units (G, S, and H units). Specifically, the basic units of lignin appeared at 152.7 ppm (etherified, $S_{3,5}$), 138.1 ppm (etherified, S_4), 134.4 to 134.7 ppm (etherified, S_1 or G_1), 133.4 ppm (nonetherified, S_1 and G_1), 106.8 ppm (oxidized, $S'_{2,6}$), 104.3 ppm ($S_{2,6}$), 149.7 (etherified, G_3), 148.0 ppm (nonetherified G_3 or nonetherified $S_{3,5}$), 145.5 ppm (nonetherified G_4), 119.8 (etherified and nonetherified G_6), 114.8 (etherified and nonetherified G_5), and 128.1 ppm ($H_{2,6}$). In addition, the ^{13}C-NMR spectrum of the lignin was almost absent of typical polysaccharides (90.0 to 102.0 ppm), suggesting that the lignin fractions contained small amounts of associated polysaccharides. Furthermore, other strong signals in the ^{13}C-NMR spectrum were also detected. For instance, the signals at 168.1, 160.0, 144.3, 130.2, 125.3, 115.9, and 115.4 ppm were corresponded to C-9 (γ), C-4, C-7, C-2/C-6, C-1, C-3/C-5, and C (β) in p- coumaric acid (PCA), respectively. Moreover, the signals of ferulic acid (FA) at 168.1, 144.3, and 121.9 ppm were C-9, C-7, and C-6, respectively. In general, the spectra of the three lignin samples were similar except for different intensities of these signals. The intensity of etherified $S_{3,5}$ signals in L_1 was strong as compared with that of L_3, implying that more S-type lignin were extracted with 18% Na_2S for 140 min. Moreover, the bands between 120.0 and 140.0 ppm became weak in L_5 as compared with those in L_3, indicating that some depolymerization between lignin

units appeared at the higher degree sodium hydroxide dosage. More importantly, in this study, the C–β, C–α, and C–γ of β–*O*–4 units in the lignin fractions could be distinguished by 86.0, 71.7, and 60.1 ppm, respectively, which indicated that β–*O*–4 units were not cleaved under the given alkaline condition.

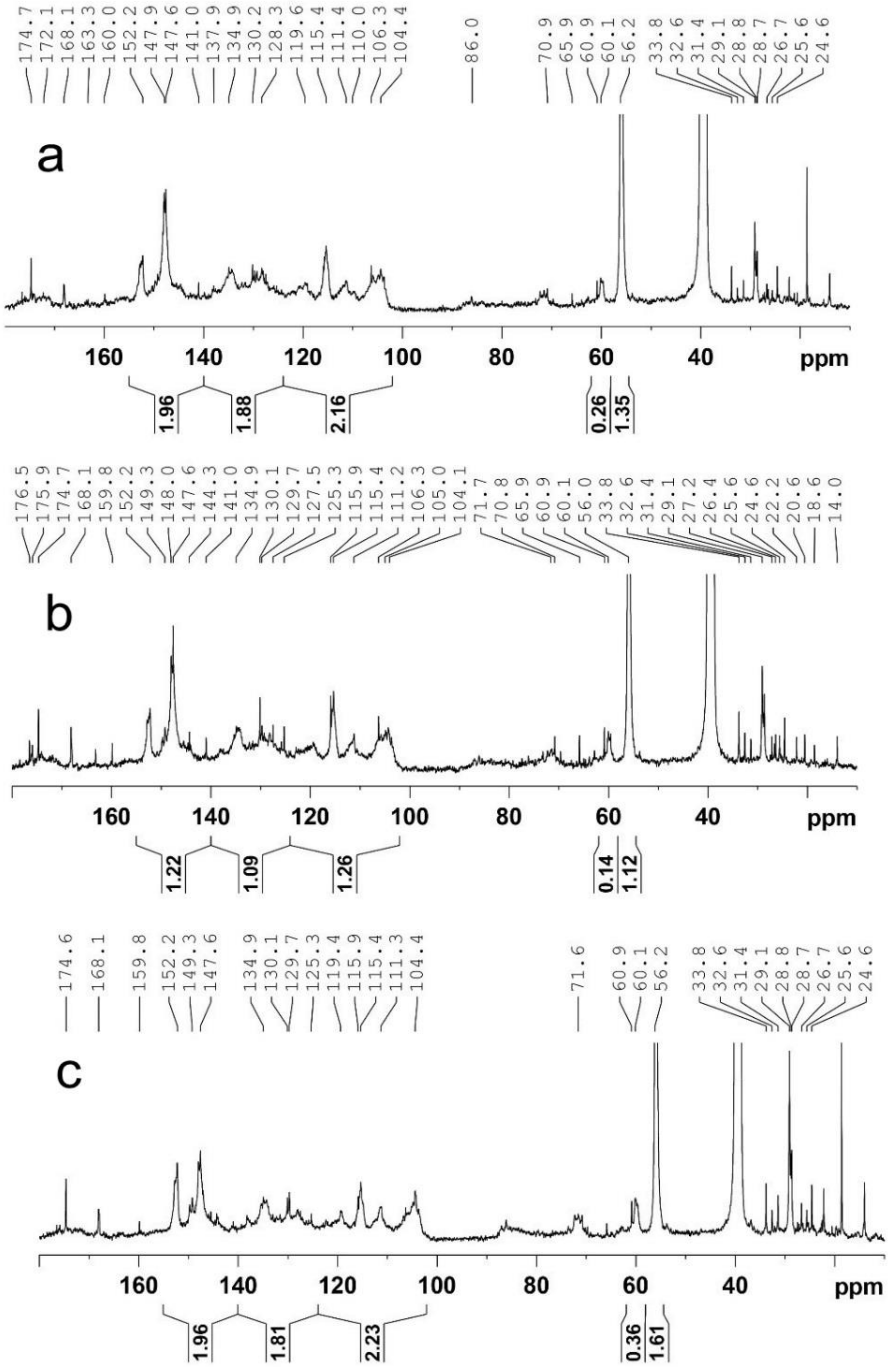

Fig. 1. ^{13}C-NMR of the lignin fractions obtained from wheat straw under different pretreatment conditions. (a) L_1 : sodium hydroxide dosage 10%, sulfidity 18%, heating time 140 min; (b) L_3 : sodium hydroxide dosage 10%, sulfidity 10%, heating time 140 min; (c) L_5 : sodium hydroxide dosage 12%, sulfidity 14%, heating time 140 min

Quantification of the lignin fractions gave more precise structural features of lignin from wheat straw (Table 4) (Martínez *et al.* 2008). Different pretreatment conditions had a slight effect on the content of the C–O linkage (integration region from 155.0 to 154.0 ppm). However, the contents of the C–C linkage (integration region from 140.0 to 124.0 ppm) were 1.88/100Ar and 1.81/100Ar in L_1 and L_5, respectively, implying that the lignin was depolymerized under a relatively high alkali concentration. In addition, the breakage of C–C linkages generated more C–H linkages. The content of β-*O*-4 linkage increased under the severe pretreatment conditions (high concentration of alkali or high degree of vulcanization) because the higher ratio of S-type lignin was extracted. In other words, the extracted S-type lignin contained more β–*O*–4 linkage content. In contrast, the content of OCH_3 decreased from 1.35/Ar in L_1 to 1.12/Ar in L_3, suggesting that demethoxylation occurred at the higher alkaline concentration. Considering the higher S content, which was calculated from 2D-HSQC of L_3, it was concluded that demethoxylation preferentially took place in G units at 10% NaOH conditions.

Table 4. Quantification of the Lignin Fractions by the Quantitative ^{13}C-NMR Method

δ (ppm)	Assignment	L_1	L_3	L_5
155-140	Aromatic C–O	1.96	1.22	1.96
140-124	Aromatic C–C	1.88	1.09	1.81
124-102	Aromatic C–H	2.16	1.26	2.23
62-58.1	*β-O*-4 linkages	0.26	0.14	0.36
58.1-54.5	CH_3O	1.35	1.12	1.61

[a] Results expressed per one Ar based on quantitative ^{13}C-NMR spectra

2D-HSQC NMR Spectra

2D-HSQC spectroscopy is a powerful tool for the determination and quantitative analysis of lignin structures. To further illustrate the structural features of lignins, the lignin samples of L_1, L_3, L_5, L_{11}, and L_{13} were investigated by 2D-HSQC NMR spectra. As shown in Figs. 2 and 3, the HSQC NMR spectra of the lignin fractions exhibited aliphatic (C/H 10–40/0.5–2.5) and aromatic ^{13}C–^{1}H correlation regions (C/H 95–150/5.5–8.0). The main cross signals of the lignin fractions in the HSQC spectra are assigned in Table 5 according to previous reports (Rencoret *et al.* 2011; Sun *et al.* 2013).

The obvious signal of C_α–H_α correlations in β–*O*–4 substructures was observed in all the lignin factions at δ_C/δ_H 71.6/4.86, whereas the C_γ–H_γ correlations in β–*O*–4 substructures were located at δ_C/δ_H 60.3/3.38. The C_β–H_β correlations at δ_C/δ_H 83.8/4.29 and 85.8/4.12 linked to G/H and S lignin units in β–*O*–4 substructures, respectively. In addition, the β–β substructures with different intensity signals were also observed in the HSQC spectra. The signals were detected with their C_α–H_α, C_β–H_β, and double C_γ–H_γ correlations at δ_C/δ_H 84.9/4.62, 53.5/3.07, and 71.0/4.15 (3.79), respectively. However, the signal of phenylcoumaran (β–5) substructures for $C_{\alpha–\alpha}$ correlations was only detected at δ_C/δ_H 87.1/5.50 in L_{13}.

In the aromatic region, syringyl (S), guaiacyl (G), and *p*-hydroxyphenyl (H) units showed prominent correlations at δ_C/δ_H 103.9/6.72 ($S_{2,6}$), 111.0/6.98 (G_2), 115.0/6.75 (G_5), 118.7/6.81 (G_6), and 128.5/7.20 ($H_{2,6}$), respectively (Fig. 3). Varying degrees of oxidized syringyl units were detected due to the presence of a correlation at δ_C/δ_H 105.8/7.25 ($S'_{2,6}$). In addition, the dissociated PCA_8 (C_8–H_8) correlations were located at δ_C/δ_H 115.4/6.30. However, the signals corresponding to PCA_8 were not detected in the lignin fractions of L_1

and L_{11}. Furthermore, the cross-signals of correlations $C_{2,6}$–$H_{2,6}$, $C_{3,5}$–$H_{3,5}$, and C_7-–H_7 in dissociated PCA were observed at δ_C/δ_H 129.8/7.51, 115.4/6.79, and 143.8/7.49, respectively. Likewise, the FA_2 (C_2–H_2), FA_8 (C_8–H_8), and FA_7 (C_7–H_7) correlations were observed at δ_C/δ_H 111.0/7.28, 116.4/6.40, and 143.7/7.50.

Table 5. Assignments of ^{13}C–^{1}H Cross-Signals in HSQC Spectra of Lignin Fraction from Wheat Straw

Label	δ_C/δ_H (ppm)	Assignment
B_β	53.5/3.07	C_β–H_β in *β*–*β* (resinol) substructures (B)
OMe	55.6/3.74	C–H in methoxyls
A_γ	60.3/3.38	C_γ–H_γ in *β*–*O*–4 substructures (A)
F_γ	61.2/4.09	C_γ–H_γ in *p*-hydroxycinnamyl alcohol end groups (F)
C_γ	62.2/3.60	C_γ–H_γ in phenylcoumaran substructures (C)
B_γ	71.0/3.79-4.15	C_γ–H_γ in *β*–*β* resinol substructures (B)
A_α	71.6/4.86	C_α–H_α in *β*–*O*–4 linked to a S unit (A)
$A_{\beta(G/H)}$	83.8/4.29	C_β–H_β in *β*–*O*–4 linked to G unit (A)
B_α	84.9/4.62	C_α-–H_α in *β*–*β* resinol substructures (B)
$A_{\beta(S)}$	85.8/4.11	C_β–H_β in *β*–*O*–4 linked to a S unit (A)
C_α	87.1/5.50	C_α–H_α in phenylcoumaran substructures (C)
$S_{2,6}$	103.9/6.72	$C_{2,6}$–$H_{2,6}$ in syringyl units (S)
$S'_{2,6}$	105.8/7.25	$C_{2,6}$–$H_{2,6}$ in oxidized S units (S′)
FA_2	111.0/7.28	C_2–H_2 in ferulic acid (FA)
G_2	111.0/6.98	C_2–H_2 in guaiacyl units (G)
PCA_8	115.0/6.30	C_8–H_8 in p-coumaric acid (PCA)
G_5	115.0/6.70	C_5-H_5 in guaiacyl units (G)
$PCA_{3,5}$	115.0/6.87	$C_{3,5}$–$H_{3,5}$ in p-coumaric acid (PCA)
FA_8	116.4/6.40	C_8–H_8 in ferulic acid (FA)
G_6	118.7/6.81	C_6–H_6 in guaiacyl units (G)
FA_6	121.9/7.09	C_6–H_6 in ferulic acid (FA)
$H_{2,6}$	128.5/7.20	$C_{\alpha\beta}$–$H_{\alpha\beta}$ in stilbenes units
$PCA_{2,6}$	129.7/7.50	$C_{2,6}$–$H_{2,6}$ in *p*-coumaric acid (PCA)
PCA_7	143.7/7.50	C_7–H_7 in *p*-coumaric acid (PCA)

Based on the quantification methodology (Rencoret *et al.* 2011; Sun *et al.* 2013), the main substructures among the lignin fractions and their abundances were estimated quantitatively. As shown in Table 6, the ratio of S/G/H was used to estimate the difference of lignin fractions in different conditions. For example, the ratios of L_1 and L_3 were 43/48/9 and 56/41/3, respectively.

Table 6. Quantification of the Lignin Fractions by Quantitative 2D-HSQC NMR

Sample	S/G/H	*β*-*O*-4	*β*-*β*	*β*-5	$PCA_{2,6}$	FA_2
L_1	43/48/9	8.76	0.47	1.67	0.83	9.99
L_3	56/41/3	13.94	2.63	ND	5.59	7.59
L_5	46/48/5	5.76	1.38	ND	4.64	9.37
L_{11}	47/48/5	33.15	3.07	1.57	6.89	15.49
L_{13}	47/51/2	16.02	1.35	ND	3.17	9.58

[a] Results expressed per 100 Ar based on quantitative 2D-HSQC spectra

[b] S/G/H ratio obtained by the equation: S/G/H ratio = 0.5I ($S_{2,6}$) / I (G_2)/ 0.5I ($H_{2,6}$)

[c] Not detectable

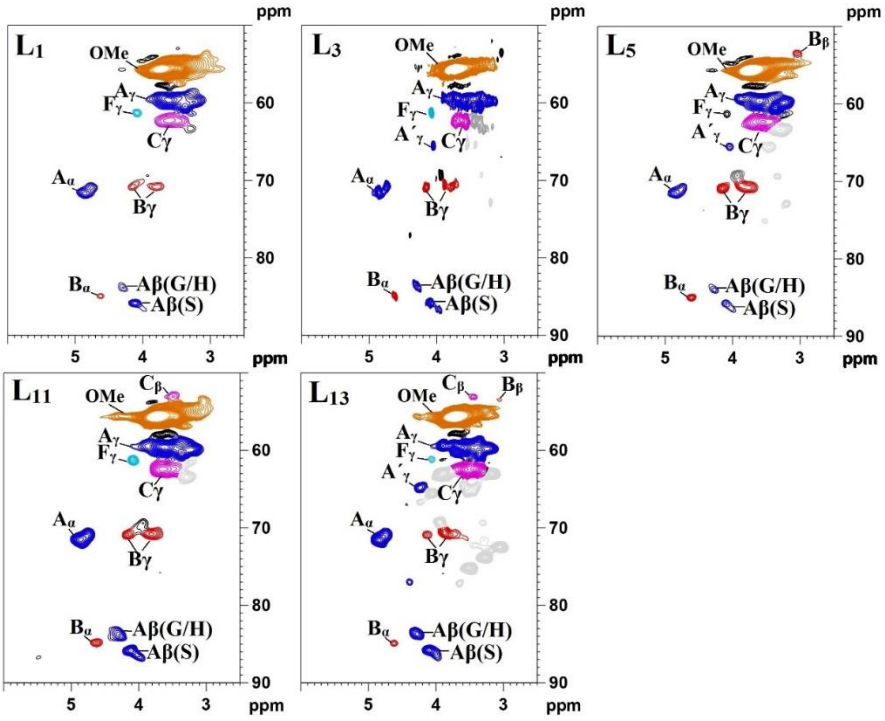

Fig. 2. 2D-HSQC spectra (side-chain region) of the lignin samples obtained from wheat straw

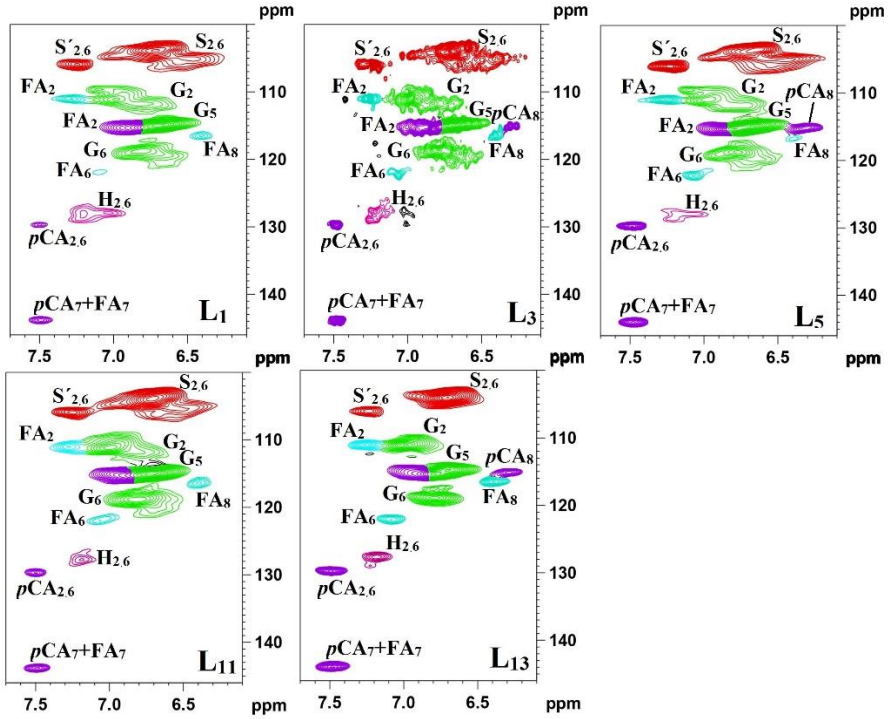

Fig. 3. 2D-HSQC spectra (aromatic regions) of the lignin sample

The high S/G/H ratio indicated that the S-type lignin fractions were more easily released than the G-type lignin fractions (Sun *et al.* 2013). For the S/G/H ratio, it could be also concluded that the lignin extracted from wheat straw was an HGS type, which had

predominant amounts of G and S units together with a minor proportion of H units.

For the β–*O*–4 linkage, the relative contents in L_1 and L_3 were 8.76/100Ar and 13.94/100Ar, respectively. The reason for this increase was possibly that more S-type lignin fractions were released under the condition of high alkali concentration, which could be reflected by the high S/G/H ratio (56/41/3 *versus* 43/48/9). However, the content of β–*O*–4 linkages decreased to 5.76/100Ar in L_5, suggesting that the β–*O*–4 linkage was more easily cleaved in the alkali concentration of 14%. In addition, the extension of the pretreatment time from 60 to 120 min resulted in an obvious decrease in the content of β–*O*–4 linkages. Therefore, it can be concluded that the β–*O*–4 linkage was more easily ruptured under harsh pretreatment conditions.

Besides the cleavage of the β–*O*–4 aryl ether linkage, the prominent structural alterations of β–β and β–5 linkages were also observed after the pretreatment process. The relative content of β–β linkages in L_3 was enhanced as compared to that of L_1, suggesting that more carbon-carbon linkages were formed in the higher alkaline concentration (10%). However, the content of β–β linkages decreased to 1.38/100 Ar in the alkaline concentration of 14% (L_5), indicating that a partial depolymerization of lignin occurred during the treatment with a higher concentration of alkaline. In addition, the content of β–β linkages decreased from 3.07 to 1.35/100/Ar with an increase in time from 60 to 100 min. The β–5 linkage, however, seemed unstable as compared with β–5 and β–*O*–4 linkages, and it was not easily detected in the 2D-HSQC spectra of L_3, L_5, and L_{13}. The reason for the decrease of the signal intensity in β–5 linkages was probably that the resolution of 2D-HSQC NMR was largely reduced for condensed lignin so that newly formed β–5 linkages were generally less detectable in 2D-HSQC NMR than that in C-13 NMR.

In addition to the cleavage of β–*O*–4 aryl ether linkages and the degradation or condensation of carbon-carbon linkages, the PCA/FA ratio was also an important parameter when investigating the structural transformation of lignin. The differences in the ratios of PCA/FA were probably caused by the different treatment conditions, and the ratio of PCA/FA rapidly increased from 0.08 (L_1) to 0.74 (L_3). This increase suggested that most of the etherified FA was removed and the increment of alkali concentration increased from 6% to 10%. As the concentration of alkali further increased to 14%, however, the PCA/FA ratio increased to 0.94 (L_5). In contrast, the ratio of PCA/FA decreased when the treated time increased from 60 to 100 min, and increased again when the treated time was 120 min.

^{31}P-NMR Spectral Analysis

To further investigate the functional hydroxyl of the lignin obtained from wheat straw, a quantitative ^{31}P-NMR technique was applied (Fig. 4 and Table 7) (Pu *et al.* 2011). The signals of the aliphatic hydroxyl and carboxyl group in the lignin were located in the ranges 146.0 to 149.0 and 134.5 to 134.2 ppm, respectively. The peaks of the guaiacyl phenolic OH (G–OH) and the syringyl phenolic OH (S–OH) were separately located from 138.8 to 140.2 and 142.2 to 143 ppm, respectively. The signals of condensed phenolic OH (5-substitued OH) for G-type lignin located from 141.4 to 142.2 ppm. The content of aliphatic OH of the L_5 decreased from 2.22 (L_3) to 2.18 mmol/g (L_5) as the alkali concentration increased from 6% to 14%, which could have resulted from the dehydration reaction in the side-chain of lignin. The decrease of aliphatic OH content in L_5 likely occurred because the oxidization happened under harsh conditions, reflected by the increasing of carboxylic group content. In addition, the content of S-type OH was less than that of the corresponding G-type OH in all the lignin fractions, implying that the majority of S-type lignin was involved in forming the β–*O*–4 linkages, and only a small amount of

S-type OH could be detected by the ^{31}P-NMR technique. Additionally, the low content of total phenolic OH in L_5 and L_{13} suggested that the lignin extracted under the harsh conditions may have more etherified lignin units owing to the formation of phenyl glycoside linkages (Granata and Argyropoulos 1995).

Table 7. Quantitative ^{31}P-NMR of the Lignin Fractions (mmol/g)

Sample	Aliphatic OH	Syringyl OH	Guaiacyl OH		*p*-Hydroxyphenyl OH + PCA-OH	Carboxylic Group	Total Phenolic OH
			C[a]	NC[b]			
L_1	2.23	1.27	0.37	1.15	0.37	1.04	3.16
L_3	2.21	0.97	0.34	0.99	0.32	1.05	2.62
L_5	2.18	1.01	0.32	1.00	0.28	1.51	2.61
L_{11}	3.29	0.90	0.30	0.92	0.23	1.04	2.35
L_{13}	3.64	0.40	0.19	0.73	0.29	1.19	1.61

[a] Condensed
[b] Noncondensed
PCA-OH, free *p*-coumaric acid

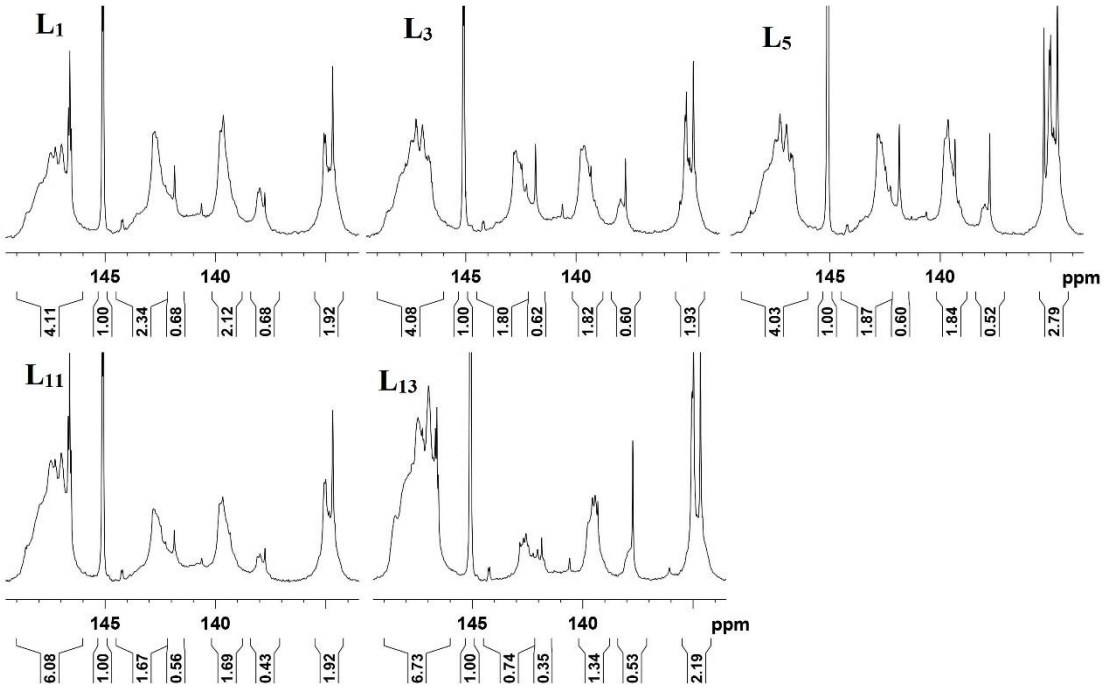

Fig. 4. ^{31}P spectra of the lignin samples obtained from wheat straw

CONCLUSIONS

1. The lignin fractions obtained from wheat straw were typical grass lignin that contained primarily S and G units, as well as small amounts of H units. The lignin fractions were mainly composed of β–*O*–4 aryl ether linkages, followed by lower amounts of β–β and β–5 linkages.

2. The lignin fractions obtained at mild conditions were rich in β–*O*–4 linkages, which were particularly important for their subsequent utilization, such as degradation into chemicals and modification into materials. Molecular weight and NMR analysis indicated that the different treatment conditions not only enhanced the lignin depolymerization but also promoted lignin condensation. The alkali concentration, sulfurizing degree, and treatment temperature were synergistically critical in the depolymerization of lignin.

ACKNOWLEDGMENTS

The authors are grateful for the support of the China Postdoctoral Science Foundation (2016M602472), the National Natural Science Foundation of China (No. 31600471), the Natural Science Foundation of Guangdong Province (2015A030310369), the Foundation (NO. 2016QN02) of State Key Laboratory of Pulp and Paper Engineering (South China University of Technology), and 111 Plan and Guangdong Provincial Science and Technology Plan Projects (Number: 2015B020241001, Name: Research and Application of Biomass Pretreatment and Ethanol Production Technology).

REFERENCES CITED

Balat, M., and Balat, H. (2009). "Recent trends in global production and utilization of bio-ethanol fuel," *Applied Energy* 86(11), 2273-2282. DOI: 10.1016/j.apenergy.2009.03.015

Boateng, A., Weimer, P. J., Jung, H. G., and Lamb, J. F. S. (2008). "Response of thermochemical and biochemical conversion processes to lignin concentration in alfalfa stems," *Energy & Fuels* 22(4), 2810-2815. DOI: 10.1021/ef800176x

Bouxin, F. P., McVeigh A., Tran F., Westwood N. J., Jarvis M. C., and Jackson S. D. (2015). "Catalytic depolymerisation of isolated lignins to fine chemicals using a Pt/alumina catalyst: Part 1 - Impact of the lignin structure," *Green Chem* 17, 1235-1242. DOI: 10.1039/C4GC01678E

Del Río, J. C., Rencoret, J., Marques, G., Li, J., Gellerstedt, G., Jiménez-Barbero, J., Martínez, A. T., and Gutiérrez, A. (2009). "Structural characterization of the lignin from jute (*Corchorus capsularis*) fibers," *Journal of Agricultural & Food Chemistry* 57(21), 10271-10281. DOI: 10.1021/ jf900815x

Duval, A., and Lawoko, M. (2014). "A review on lignin-based polymeric, micro-and nano-structured materials," *Reactive and Functional Polymers* 85, 78-96. DOI: 10.1016/j.reactfunctpolym.2014.09.017

Gandini, A. (2008). "Polymers from renewable resources: a challenge for the future of macromolecular materials," *Macromolecules* 41(24), 9491-9504. DOI: 10.1021/ma801735u

Granata, A., and Argyropoulos, D. S. (1995). "2-chloro-4,4,5,5-tetramethyl-1,3,2-dioxaphospholane, a reagent for the accurate determination of the uncondensed and condensed phenolic moieties in lignins," *Journal of Agricultural & Food Chemistry* 43(6), 1538-1544. DOI: 10.1021/jf00054a023

Holtman, K. M., Chang, H. M., Jameel, H., and Kadla, J. F. (2006). "Quantitative ^{13}C NMR characterization of milled wood lignins isolated by different milling

techniques," *Journal of Wood Chemistry & Technology* 26, 21-34. DOI: 10.1080/02773810600582152

Kapoor, M., Raj, T., Vijayaraj, M., Chopra, A., Gupta, R. P., Tuli, D. K., and Kumar, R. (2015). "Structural features of dilute acid, steam exploded, and alkali pretreated mustard stalk and their impact on enzymatic hydrolysis," *Carbohydrate Polymers* 124, 265-273. DOI: 10.1016/j.carbpol.2015.02.044

Kumar, D., and Murthy, G. S. (2013). "Stochastic molecular model of enzymatic hydrolysis of cellulose for ethanol production," *Biotechnology for Biofuels* 6(63), 1-20. DOI: 10.1186/1754-6834-6-63

Liu, S., Lu, H., Hu, R., Shupe, A., Lu, L., and Liang, B. (2012). "A sustainable woody biomass biorefinery," *Biotechnology Advances* 30(4), 785-810. DOI: 10.1016/j.biotechadv.2012.01.013

Lu, F., and Ralph, J. (2011). "Solution-state NMR of lignocellulosic biomass," *Journal of Biobased Materials and Bioenergy* 5(2), 169-180. DOI: 10.1166/jbmb.2011.1131

Martínez, Á. T., Rencoret, J., Marques, G., Gutiérrez, A., Ibarra, D., Jiménez-Barbero, J., and del Río, J. C. (2008). "Monolignol acylation and lignin structure in some nonwoody plants: A 2D NMR study," *Phytochemistry* 69, 2831-2843. DOI: 10.1016/j.phytochem.2008.09.005

Pu, Y., Cao, S., and Ragauskas, A. J. (2011). "Application of quantitative ^{31}P NMR in biomass lignin and biofuel precursors characterization," *Energy & Environmental Science* 4, 3154-3166. DOI: 10.1039/C1EE01201K

Rencoret, J., Gutiérrez, A., Nieto, L., Jiménez-Barbero, J., Faulds, C. B., Kim, H., Ralph, J., Martínez, Á. T., and del Río, J. C. (2011). "Lignin composition and structure in young versus adult *Eucalyptus globulus* plants," *Plant Physiology* 155(2), 667-682. DOI: 10.1104/pp.110.167254

Rencoret, J., Marques, G., Gutierrez, A., Ibarra, D., Li, J., Gellerstedt, G., Santos, J. I., Jiménez-Barbero, J., Martinez, A. T., and del Rio, J. C. (2008). "Structural characterization of milled wood lignins from different eucalypt species," *Holzforschung* 62(5), 514-526. DOI: 10.1515/HF.2008.096

Saini, J. K., Agrawal, R., Satlewal, A., Saini, R., Gupta, R., Mathur, A., and Tuli, D. (2015). "Second generation bioethanol production at high gravity of pilot-scale pretreated wheat straw employing newly isolated thermotolerant yeast *Kluyveromyces marxianus* DBTIOC-35," *RSC Advances* 5(47), 37485-37494. DOI: 10.1039/c5ra05792b

Stark, A. (2011). "Ionic liquids in the biorefinery: A critical assessment of their potential," *Energy & Environmental Science* 4, 19-32. DOI: 10.1039/C0EE00246A

Stewart, D. (2008). "Lignin as a base material for materials applications: Chemistry, application and economics," *Industrial Crops & Products* 27(2), 202-207. DOI: 10.1016/j.indcrop.2007.07.008

Sun, R. C., and Tomkinson, J. (2002). "Comparative study of lignins isolated by alkali and ultrasound-assisted alkali extractions from wheat straw," *Ultrasonics Sonochemistry* 9(2), 85-93. DOI: 10.1016/S1350-4177(01)00106-7

Sun, R. C., Fang, J. M., and Tomkinson, J. (2000a). "Delignification of rye straw using hydrogen peroxide," *Industrial Crops & Products* 12(2), 71-83. DOI: 10.1016/S0926-6690(00)00039-X

Sun, R. C., Tomkinson, J., Zhu, W., and Wang, S. Q. (2000b). "Delignification of maize stems by peroxymonosulfuric acid, peroxyformic acid, peracetic acid, and hydrogen peroxide. 1. Physicochemical and structural characterization of the solubilized

lignins," *Journal of Agricultural & Food Chemistry* 48(4), 1253-1262. DOI: 10.1021/jf990646e

Sun, S. L., Wen, J. L., Ma, M. G., and Sun, R. C. (2014). "Structural elucidation of sorghum lignins from an integrated biorefinery process based on hydrothermal and alkaline treatments," *Journal of Agricultural & Food Chemistry* 62(32), 8120-8128. DOI: 10.1021/jf501669r

Sun, S. L., Wen, J. L., Ma, M. G., Li, M. F., and Sun, R. C. (2013). "Revealing the structural inhomogeneity of lignins from sweet sorghum stem by successive alkali extractions," *Journal of Agricultural & Food Chemistry* 61(18), 4226-4235. DOI: 10.1021/jf400824p

Tuck, C. O., Pérez, E., Horváth, I. T., Sheldon, R. A., and Poliakoff, M. (2012). "Valorization of biomass: Deriving more value from waste," *Science* 337(6095), 695-699. DOI: 10.1126/science.1218930

Upton, B. M., and Kasko, A. M. (2015). "Strategies for the conversion of lignin to high-value polymeric materials: Review and perspective," *Chemical Reviews* 116(4), 2275-2306. DOI: 10.1021/acs.chemrev.5b00345

Wang, C., Kelley, S. S., and Venditti, R. A. (2016). "Lignin-based thermoplastic materials," *ChemSusChem* 9(8), 770-783. DOI: 10.1002/cssc.201501531

Zeng, J., Helms, G. L., Gao, X., and Chen, S. (2013). "Quantification of wheat straw lignin structure by comprehensive NMR analysis," *Journal of Agricultural & Food Chemistry* 61(46), 10848-10857. DOI: 10.1021/jf4030486

Zhang, Z., Harrison, M. D., Rackemann, D. W., Doherty, W. O. S., and O'Hara, I. M. (2016). "Organosolv pretreatment of plant biomass for enhanced enzymatic saccharification," *Green Chemistry* 18(2), 360-381. DOI: 10.1039/C5GC02034D

Article submitted: November 14, 2016; Peer review completed: January 7, 2017; Revised version received: January 16, 2017; Accepted: January 17, 2017; Published: February 10, 2017.
DOI: 10.15376/biores.12.2.2407-2420